

EXPERIMENTAL CHARACTERIZATION AND 3D MODELING OF CARBON/CARBON COMPOSITES OXIDATION : ROLE OF THE INTERPHASE

Jean Lachaud*, Yvan Aspa, Gérard L. Vignoles, Gwénaél Bourget

Laboratoire des Composites ThermoStructuraux, UMR 5801 : CNRS-SAFRAN-CEA-UB1,
Domaine Universitaire de Bordeaux – 3, Allée de La Boétie, 33600 Pessac, France

*(corresponding author : jean.lachaud@gadz.org)

ABSTRACT

This work aims to explain the oxidation behavior of a 3D C/C composite yarn. First, SEM analyses of samples submitted to repeatable oxidation tests stopped at different oxidation stages have provided the basis of the study: the interphase lying between the fibers and the matrix is a weak phase. Then, a reaction/diffusion model has been set up and solved analytically in steady state. The outputs are (i) the morphology of surface roughness features (represented as a function of the physico-chemical parameters), (ii) the effective reaction rate of the material (derived from those of its components). The effective reactivity of a yarn in the composite is shown to follow a complex mixture law. The oxidation rates of the composite components are derived from a topological analysis of the surface roughness features. Finally, a 3D numerical simulation featuring transient regime gives results in agreement with experimental observations.

1. INTRODUCTION

The oxidation resistance of carbon/carbon (C/C) composites has been widely studied in the last decades. Several experimental results have shown the non trivial behavior of these heterogeneous materials during vaporization [1]. Indeed, a typical composite surface roughness develops on the reacting wall until it reaches a steady state. This surface roughness leads to a composite behavior which has a strong effect on the global oxidation resistance. The effective oxidation rate of the composite can not be modeled using a simple arithmetic average of the oxidation rates of its components [2]. Moreover, in the yarns perpendicular to the interface, the surface roughness onset is mainly driven by the presence of a weak phase : the interface lying between the fibers and the intra-yarn matrix. This work aims to understand and explain the complex oxidation process of the material through an experimental and a modeling study.

2. EXPERIMENTS AND MATERIAL ANALYSIS

Repeatable experiments have been carried out in a cylindrical oxidation reactor at a controlled temperature (625°C) under dry air at atmospheric pressure. The reactor section is a 14 mm diameter half-disk. Its effective length is 30 cm. The sample is reduced to a 1 cm² square surface incorporated in the center of the lower wall of the reactor (see figure 1). The average velocity of the flow is 1 m.s⁻¹. This value has been chosen to ensure a high laminar oxygen injection flow. The global scale modeling is addressed in a companion work; the reactor has been modeled and the model has been solved using Fluent 6 [3]. The Péclet mass number close to the sample is shown to be low, *i.e.* the advection velocity close to the sample is negligible when compared

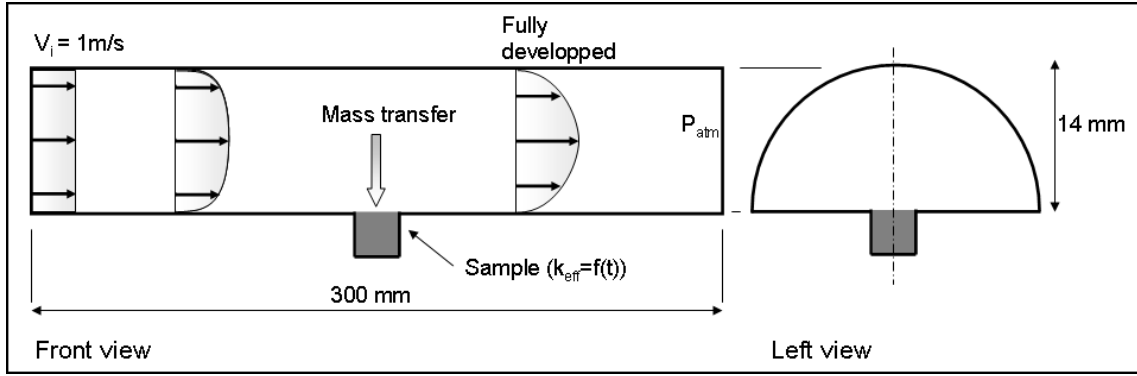


Figure 1: Oxidation reactor geometry and experimental conditions (dry air at $T = 625^{\circ}\text{C}$, $P = 1\text{atm}$).

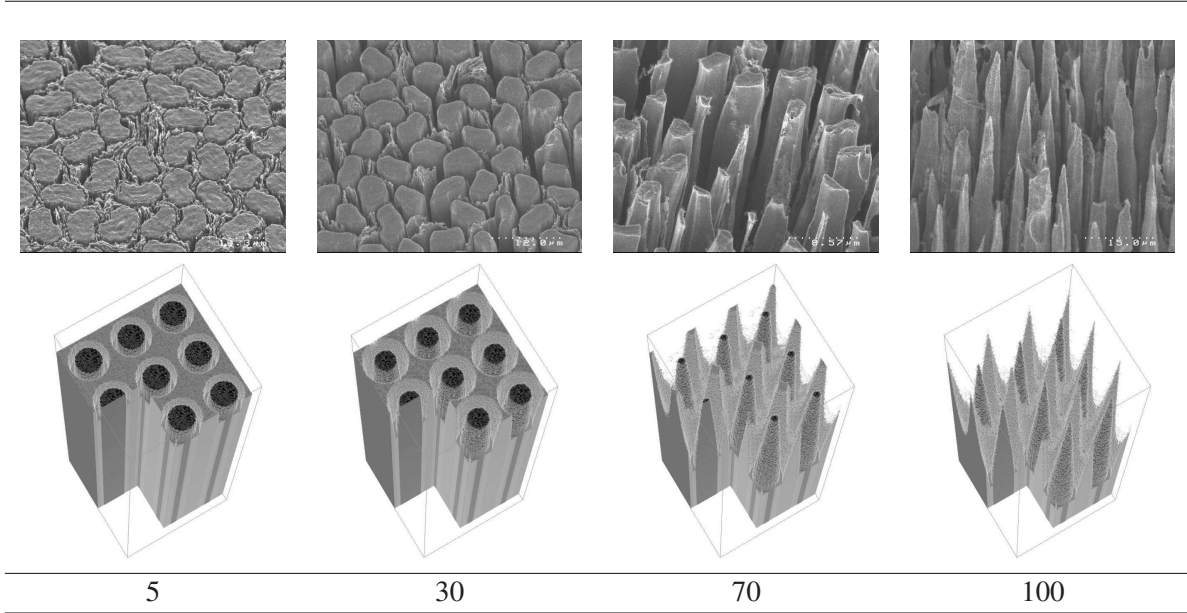


Figure 2: Experimental behavior and simulation results as a fonction of h_f (μm).

to the mass diffusion velocity. The boundary layer is not fully developed on the sample. It enables a larger mass transfer by diffusion as the boundary layer is small. These conditions promote a reaction limited mass transfer in the bulk fluid phase. However, it is shown that this condition is not sufficient to provide a reaction limited mass transfer at local scale everywhere on the fluid/composite interface. The temperature gradient in the inner part of the oxidation reactor is negligible.

The material tested is a 3D carbon/carbon composite fabricated from a 3D ex-PAN carbon fiber woven preform compregnated by a pitch-based carbon matrix, then carbonized and graphitized. Scanning electron microscopy (SEM) analyses performed on this 3D C/C after a short oxidation test clearly show the presence of a more reactive interphase lying between the fibers and the intra-yarn matrix (see top-left micrograph of figure 2). This interphase is about $1\mu\text{m}$ thick. This phenomenon has already been described by Labruquère [1] for a carbon/carbon composite made of an ex-PAN preform and a CVI grown pyrocarbon matrix. 002C dark field measurement has been done by transmission electron microscopy (TEM): the pyrocarbon has been shown to be granular at the interphase and smooth laminar in the bulk matrix phase. The granular pyrocarbon is known to be a less organized and chemically resistant turbostratic carbon than the smooth

laminar form [1]. Consequently the interphase is submitted to a preferential vaporisation and recession.

The micrographs of figure 2 suggest that the oxidation rates of the matrix and of the fibers are low when compared to those of the interphase, as these two phases recess at the same vertical velocity in transient regime while the interphase recession is higher. The oxidation rates of the ex-PAN fibers and of the pitch-based graphitized matrix have been measured independently in the oxidation reactor described above. The 3D computation [3] shows the material vaporization rate is a complex function of the mass diffusion transfer in the bulk fluid phase and of the effective reactivity of the material. In this case, the oxidation rates measured are underestimations of the actual rates. Using simulation and inverse analysis, the effective oxidation rates obtained for the matrix and the fibers are shown to be of the same order of magnitude. As a first approach, they are considered equal in this work. However, the interphase oxidation rate cannot be measured directly from mass loss study as it solely takes place inside the composite. This work enables to evaluate its value by a topological study and an inverse analysis (see subsection 4.3.).

The micrographs of figure 2 represent the morphological evolution of a yarn perpendicular to the surface typical of C/C composite vaporization. Due to an important recession of this weak interphase, the fibers, which are less reactive, are partially stripped, become thinner, and acquire a needle shape. The bulk matrix phase first acquires a ring-shaped morphology. Then it also becomes thinner, and acquires a needle shape.

3. MODEL SET-UP

This evolution has been sketched in 2D by Han [4], but it has not been modeled. In this part, a reaction/mass diffusion model is proposed to explain the phenomenon described above; then, this model is solved analytically in steady state. The oxidation rate of the interphase is evaluated through comparisons of experimental morphologies in steady state regime with the results of the model. Then, the transient regime of the surface roughness onset is simulated using a 3D numerical simulation code.

As specified in the previous section, the C/C composite yarns are heterogeneous. They are made of fibers, matrix and interphase, which are assumed homogeneous and isotropic. At 625°C, the overall chemical balance of the oxidation process can be written :



where the oxidation rates of the fibers and the matrix (noted k_{fm}) are lower than for the interphase (noted k_i). The chemical reaction is restricted to the surface. Thermal gradients induced by reaction enthalpy are negligible [5]. Mass loss is strongly coupled to mass transfer between the bulk fluid phase and the wall. As the mass Péclet number is low (see section 2), mass transfer is mainly diffusive close to the wall. A strong coupling between the global reactor modeling and the modeling of the material behavior is useless. Indeed, the global scale output is the oxidant concentration close to the wall, which is a linear factor for the material behavior [5]. Consequently, let us use a diffusive boundary layer formalism and a formal concentration C_0 for the upper boundary condition. Mass transfer is restricted to binary diffusion of the single reactant (O_2) in nitrogen.

The proposed model is sketched on Fig. 3. On this scheme the stationary rough surface is represented; however at initial time, the fluid/solid interface is flat. This profile has therefore to be obtained using a moving fluid/solid interface modeling.

Let us write mass conservation of the reactant (of molar concentration C) in the fluid phase:

$$\frac{\partial C}{\partial t} + \nabla \cdot (-D\nabla C) = 0 \quad (2)$$

Boundary conditions relative to the model domain are:

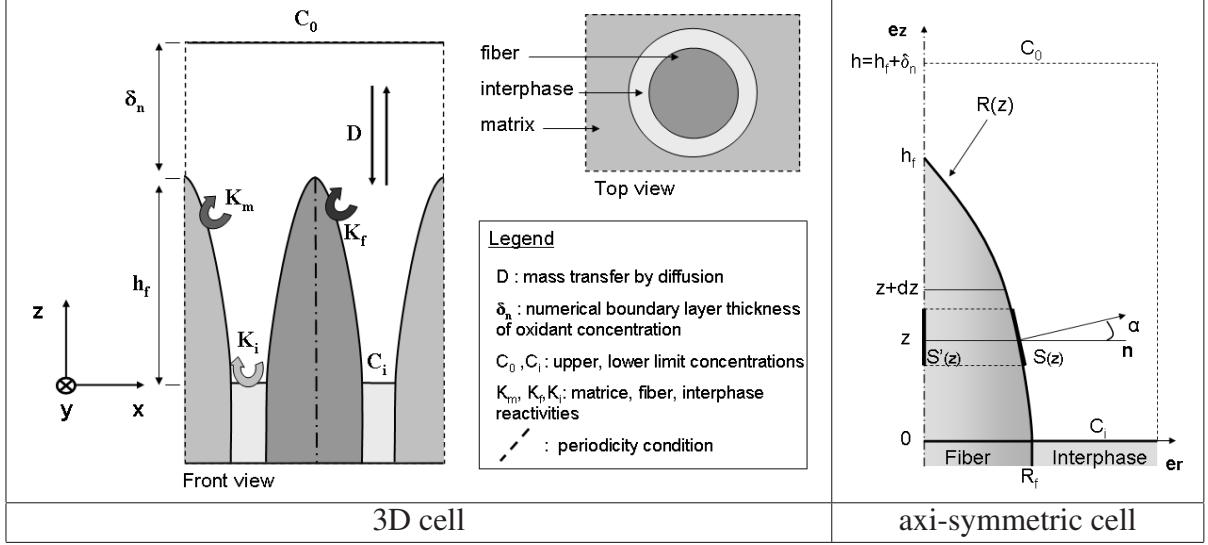


Figure 3: Scheme of the elementary pattern and of the proposed model

- On boundary layer top: $C = C_0$;
- At the fluid/solid interface the oxidation molar rate writes:

$$r = (-D\nabla C) \cdot \mathbf{n} = -k_j C \quad (3)$$

where \mathbf{n} is the normal to the surface, and k_j (m/s) the reaction kinetic constant of matrix ($j = m$), fibers ($j = f$) or interphase ($j = i$);

- Periodicity on the lateral boundaries (the yarn section is supposed infinite in transverse directions).

The interface position ($S(x, y, z, t)$) is given by the simultaneous resolution of [6]:

$$\frac{\partial S}{\partial t} + \mathbf{v} \cdot \nabla S = 0 \quad (4)$$

where $\mathbf{v} = v_s r \mathbf{n}$ is the surface local normal velocity, with v_s the solid molar volume.

4. ANALYTICAL RESULTS IN STEADY STATE

Let us solve this model analytically under the following hypotheses: (i) steady state regime onset, (ii) axi-symmetric fiber, (iii) vertical mass transfer flux in steady state, (iv) interphase surface is flat and perpendicular to the z axis. The third hypothesis has two main interests: first, it enables to address separately fiber and matrix recession (as mass transfer is decoupled for these two phases), second, the concentration profile in the cell can be derived from Fick's law. The numerical simulations performed to solve this problem have validated all these hypotheses. It also is proved the value chosen for δ_n has no influence on the simulation results.

4.1. Description of the fiber tip surface

The fiber tip surface is given by the function $R(z)$. In steady state, the increment of R between z and $z + dz$ writes:

$$R(z + dz) - R(z) = C(z) k_f v_f \frac{S(z)}{S'(z)} dt \quad (5)$$

where $S(z)$ is the surface element located at z and $S'(z)$ its projection along the z axis.

Using the vertical flux hypothesis, one can derive: $C(z) = C_i + \frac{C_0 - C_i}{h} z$; where $C_i = C_0/(1 + Da_i)$ is the reactant concentration at the interphase level, with $Da_i = k_i h/D$ the Damköhler number associated to the interphase [7].

In steady state, one has $dt = dz/\langle V_z \rangle$, where $\langle V_z \rangle = v_i k_i C_i$ is the recession velocity of the wall along \mathbf{e}_z , which is proportional to the effective oxidation rate k_i . Standard trigonometry gives:

$$\frac{S(z)}{S'(z)} = \frac{1}{\cos(\alpha)} = \sqrt{1 + \left(\frac{dR}{dz}\right)^2} \quad (6)$$

Summing up, $R(z)$ is given by the following differential equation:

$$\frac{dR}{dz} = -\frac{1 + \frac{z}{La}}{\sqrt{A^2 - \left(1 + \frac{z}{La}\right)^2}} \quad (7)$$

where $A = \frac{k_i v_i}{k_f v_f}$ and $La = D/k_i$ are respectively a dimensionless number and a length. Equation (7) is defined only for $z \in [0, La(A - 1)[$. As sketched on figure 3, the boundary condition for integration is $R(z = 0) = R_f$.

4.2. Solutions

After integration, the fiber geometry is given by:

$$R(z) = La \left(\sqrt{A^2 - \left(1 + \frac{z}{La}\right)^2} - \sqrt{A^2 - 1} \right) + R_f \quad (8)$$

with $z \in [0, La(A - 1)[$. Note that $\lim_{z \rightarrow La(A-1)} \left(\frac{dR}{dz}\right) = -\infty$, *i.e.* the slope at this point is horizontal. In other words, the fiber may exhibit a plateau (see figure 5). The equality between the recession velocity of the fiber on the plateau (V_z^f , given by the equation 9) and the matrix one (V_z) is verified for a unique fiber height $h_f = La(A - 1)$. Moreover, the global recession rate is found to be:

$$\langle V_z \rangle = V_z^f = v_f k_f C_0 \frac{1 + Da_m h_f/h}{1 - Da_m} \quad (9)$$

The reduced height h_f/R_f , which is equal to the peak-to-valley roughness (see figure 3), is an explicit function of A , and of a Sherwood number $Sh = La/R_f$:

$$\frac{h_f}{R_f} = \left(\sqrt{Sh^{-2} + 2Sh^{-1} \sqrt{A^2 - 1} - 1 - Sh^{-1}} \right) \quad (10)$$

with $Sh = R_f/La < \sqrt{A^2 - 1}$, leading to an ogival fiber. In the converse case, as explained above, the fiber tip is a plateau and $h_f = La(A - 1)$.

As represented on figure 4 for a $10 \mu\text{m}$ radius fiber, the length La is an indicator of the regime: if it tends towards zero, the recession is controlled by diffusion and there is no roughness, if it tends to infinite, then reaction controls recession, and the roughness is maximal; between these two limits the regime is intermediate. The number A is an indicator of the reactivity and density contrast between the fiber and the interphase. The higher it is, the higher h_f is, as soon as the mass diffusion process does not bring a limit.

The fiber morphology, represented on the figure 5 for $A = 5$, is a function of the Sherwood number $Sh = R_f/La$. Note that on the two schemes on the right, the plateau described above is observed.

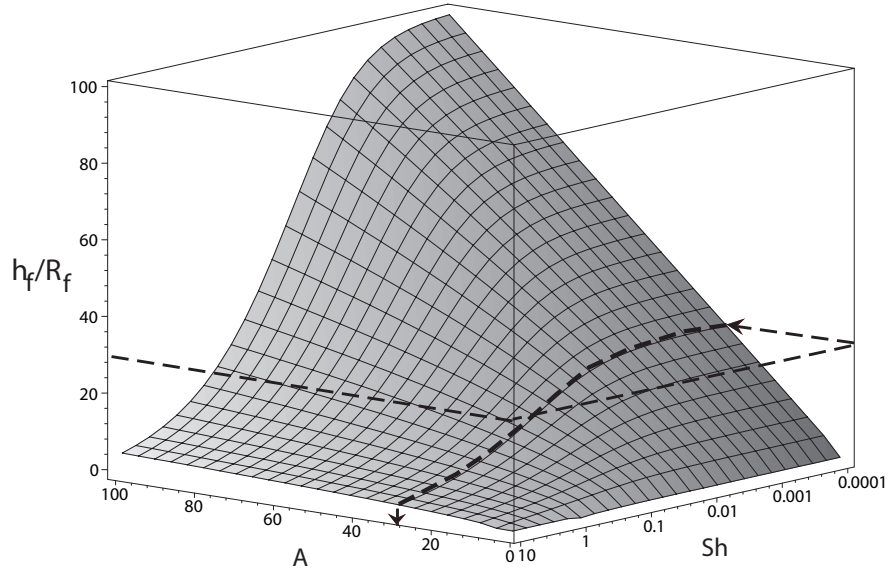


Figure 4: Plot of the reduced height h_f/R_f as a function of A and Sh .

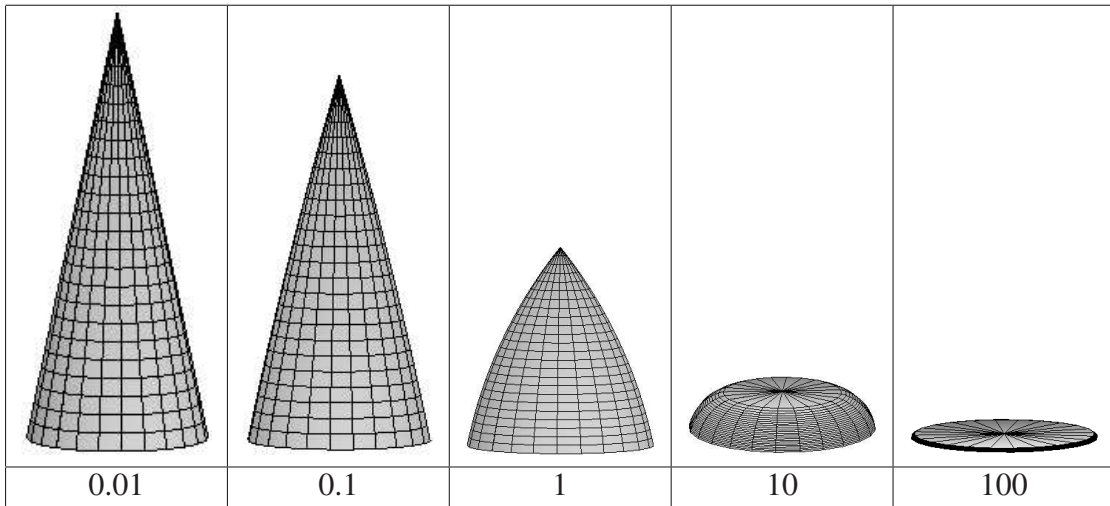


Figure 5: Fiber morphology at steady state as a function of $Sh = R_f/La$ (with $A = 5$).

When h_f is evaluated, the effective recession velocity along \mathbf{e}_z is given by :

$$\langle V_z \rangle = \frac{v_i k_i C_0}{1 + \frac{k_i(h_f + \delta_c)}{D}} \quad (11)$$

where δ_c is the concentration boundary layer thickness, which can be determined by the global modeling and 3D simulation of the oxidation reactor [3].

4.3. Inverse analysis

Let us evaluate the Sherwood number. An independent determination of k_f gives $k_f \approx 10^{-5} m.s^{-1}$. The diffusion coefficient (D) is about $1,4 \cdot 10^{-4} m^2.s^{-1}$ and the fibers radius (R_f) are around $3,5 \mu m$.

This gives $Sh = R_f/La \simeq 2,5.10^{-7}$. This low value of Sh is in agreement with the conical morphology of the fibers (see figures 2 and 5).

Relation 10 or figure 4 can be used to derive A from Sh , R_f and the experimental value of h_f . The SEM analysis shows the value of h_f lies around $100\mu m$. This gives $A \simeq 30$ which implies $k_i \simeq 3.10^{-4} m.s^{-1}$. Note that the condition $Sh = R_f/La < \sqrt{A^2 - 1}$ is verified.

5. 3D NUMERICAL SIMULATION IN TRANSIENT REGIME

Using the results of the inverse analysis, it is possible to compute the transient regime. To solve this problem in 3-D and in non-stationary regime, an efficient numerical simulation code, named AMA, has been developed on a Monte-Carlo random-walk principle. AMA, which is a C ANSI implementation, contains five main parts. (i) A 3-D image containing several phases (fluid/solids) is described by discrete cubic voxels method. (ii) The moving fluid/solid interface is determined by a simplified marching cube approach [8]. (iii) Mass transfer by diffusion is simulated by a Brownian motion simulation technique [9], which is a continuum (grid-free) and rapidly converging method to simulate diffusion in a continuous fluid. (iv) Heterogeneous first order reaction on the wall is simulated by a sticking probability (\tilde{P}) adapted to the Brownian motion simulation technique. A theoretical analysis gives [7]:

$$\tilde{P} = \frac{1}{1 + \frac{3/2\alpha D}{k\Delta r}} \quad (12)$$

The value of α (which is close to 0.8) is obtained by a numerical study [7] (v) A Dirichlet upper boundary condition is simulated using a buffer zone, where C is maintained constant.

AMA has been validated by comparison to a 1D analytical model in transient regime [7] and to the axi-symmetrical model presented above in steady state.

The transient regime has been simulated using the numerical values cited in the subsection 4.3. The steady state is reached after a computing time of 24 hours with a Xenon CPU 3.2GHz processor. The simulation results are presented on figure 2.

6. DISCUSSION

Unfortunately, it is not possible to compare the mass loss of the sample in experimental conditions with those obtained from the simulation of yarns perpendicular to surface. Indeed, the 3D C/C composite is not an unidirectional media: one has to take into account yarns parallel to the surface and parallelepipedic structural macro-pores filled with matrix. However, experimental and numerical results (carried out at a larger scale [10]) show that the steady state is reached after a duration which is principally driven by the behavior of yarns perpendicular to surface. Nevertheless, the value of h_f in the simulation results is the correct one, and the morphology of the surface state is well respected at each step of the simulation. Especially, the conical shape of the fibers is obtained (low Sherwood number).

The recession velocity (or oxidation rate) in steady state, given by equation 11, is mainly driven by the interphase recession rate in the case presented here (low Sherwood number). In other words, the fast recession of the interphase increases the surfaces of the fibers and of the matrix until they are high enough to balance the reactivity ratio $A = 30$. Consequently, in steady state regime and for a low Sherwood number, the effective reactivity turns out to be equal of the weaker phase's.

In usual conditions, the fiber-related Sherwood number is low. According to these results, the best way to improve the composite resistance to vaporisation is to reinforce the interphase.

7. CONCLUSION

The complex oxidation behavior of a 3D C/C composite yarn perpendicular to the material surface has been addressed. First, oxidation experiments have been carried out to quantify the role of the interphase lying between the fibers and the matrix. SEM observations have shown that this interphase has a vaporization rate higher than for the fibers and the matrix, which are approximatively equal. Due to an important recession of this weak interphase, the fibers, which are less reactive, are partially stripped, become thinner, and acquire a needle shape. The bulk matrix phase first acquires a ring-shaped morphology. Then it also becomes thinner, and acquires a needle shape. A reaction/diffusion model has been set up and solved analytically to explain this complex behavior and to predict its steady state morphology as a function of physical parameters. Moreover, the effective vaporization rate in steady state regime is given as a function of physical parameters and the vaporization rate of the yarn components. The comparison of SEM measurements of stripped fibers height to analytical results has provided the value of the interphase vaporisation rate. Then a 3D numerical simulation processed using AMA, a homemade simulation code, has reproduced the morphologies experimentally observed in transient regime, qualitatively and quantitatively. The study reveals that the recession rate is driven by the interphase, which is the weakest component. The next step is to study the behavior of the yarns perpendicular to the surface and to compute the effective behavior of the whole composite.

References

- [1] **S. Labruquère, X. Bourrat, R. Paillet, and R. Naslain.** Structure and oxidation of C/C composites: role of the interface. *Carbon*, 39:971–984, 2000.
- [2] **J. Lahaye, F. Louys, and P. Ehrburger.** The reactivity of carbon-carbon composites. *Carbon*, 28(1):137–141, 1990.
- [3] **N. Bertrand, J. Lachaud, F. Rebillat, and G. L. Vignoles.** Identification of intrinsic carbon fiber oxidation kinetics from experimental data and CFD modeling. In *This Conference*, 2006.
- [4] **J. C. Han, X. D. He, and S. Y. Du.** Oxidation and ablation of 3D carbon-carbon composite at up to 3000°C. *Carbon*, 33(4):473–478, 1995.
- [5] **J. Lachaud, Y. Aspa, G. L. Vignoles, and J. M. Goyhénèche.** Modélisation 3D de l’ablation thermochimique des composites C/C. In *Congrès Français de Thermique - SFT 2006*, Île de Ré, France, 16-19 May 2006.
- [6] **G. Duffa, G. L. Vignoles, J.-M. Goyhénèche, and Y. Aspa.** Ablation of C/C composites : investigation of roughness set-up from heterogeneous reactions. *International Journal of Heat and Mass Transfer*, 48(16):3387–3401, June 2005.
- [7] **J. Lachaud, G. L. Vignoles, J. M. Goyhénèche, and J. F. Epherre.** Ablation in C/C composites: microscopic observations and 3D numerical simulation of surface roughness evolution. In L. P. Cook, editor, *Thermochemistry and Metrology of Interfaces*, volume 191 of *Ceramic Transactions*. American Ceramic Society, To be published.
- [8] **G. L. Vignoles.** Modelling binary, Knudsen, and transition regime diffusion inside complex porous media. *J. of Physics IV*, C5:159–166, 1995.
- [9] **S. Torquato and I. Kim.** Efficient simulation technique to compute effective properties of heterogeneous media. *Appl. Phys. Lett.*, 55:1847–1849, 1989.
- [10] **G. Vignoles, J. Lachaud, Y. Aspa, and J. M. Goyheneche.** Ablation of carbon-based materials: multiscale roughness modeling. In *This Conference*, 2006.